



HAL
open science

Thermal shocks on an electrolytic chromium coating in a solar furnace

P. Douale, S. Serror, R. M. Pradeilles Duval, J. J. Serra, Eric Felder

► To cite this version:

P. Douale, S. Serror, R. M. Pradeilles Duval, J. J. Serra, Eric Felder. Thermal shocks on an electrolytic chromium coating in a solar furnace. *Journal de Physique*, 1999, 9 (PR3), pp.429-434. 10.1051/jp4:1999367. hal-00111635

HAL Id: hal-00111635

<https://hal.science/hal-00111635>

Submitted on 28 Apr 2018

HAL is a multi-disciplinary open access archive for the deposit and dissemination of scientific research documents, whether they are published or not. The documents may come from teaching and research institutions in France or abroad, or from public or private research centers.

L'archive ouverte pluridisciplinaire **HAL**, est destinée au dépôt et à la diffusion de documents scientifiques de niveau recherche, publiés ou non, émanant des établissements d'enseignement et de recherche français ou étrangers, des laboratoires publics ou privés.

Thermal shocks on an electrolytic chromium coating in a solar furnace

Ph. Douale, S. Serror, R.M. Pradeilles Duval, J.J. Serra* and E. Felder**

Direction des Centres d'Essais (DCE), Centre Technique d'Arcueil (CTA), 16 bis avenue Prieur de la Côte d'Or, 94114 Arcueil, France

** Groupe Haut Flux Thermique d'Odeillo (GHF), 66125 Odeillo, France*

*** Groupe Surfaces & Tribologie, Cemef, URA 1374 du CNRS, École des Mines de Paris, BP. 207, 06904 Sophia-Antipolis, France*

Abstract. The electrodeposited chromium coatings are currently used to protect surfaces in many industrial cases, such as rolling-mills, landing gear, jack rod or gun barrels. In the latter case, an important thermal effect is superimposed to the frictional one, bringing to the coating flake off. This paper presents a part of a more extended study of the damages induced in gun tubes. It deals with thermal shock resistance analysis of uncoated and chromium coated steel samples. Its aim is to reproduce and study the main damage types observed at the inner surface of gun tubes by using the DCE solar furnace in Odeillo (France). In a real weapon shooting, the thermal pulse can reach flux levels as high as 50 kW/cm^2 in an extremely brief time (about 10ms). These thermal conditions cannot be simulated at the focus of a solar furnace, so we have to determine the couple of parameters (flux level and duration) creating the same damage on the samples.

1. THE CEO SOLAR FURNACE

The 45kW Odeillo solar furnace [1] consists of three main elements :

- a/ the heliostat, a swivelling plane reflector whose function is to reflect solar radiation in an horizontal north-south direction,
- b/ the concentrator, a 10.75m focal length concave mirror covering a $10 \times 10\text{m}$ front area. Its peculiar geometry (spherical facets with a radius of curvature double that of the structure on which they are mounted) confers on the focal zone a quasi-constant ($\pm 5\%$) energy distribution over 50mm diameter circle.
- c/ the solar radiation modulating system, comprising :
 - a group of slow moving flux prevention doors and curtains whose positions remain fixed for the duration of a test,
 - a fast flux attenuator consisting of twenty shutters moving round their vertical axis and acting like venetian blind.

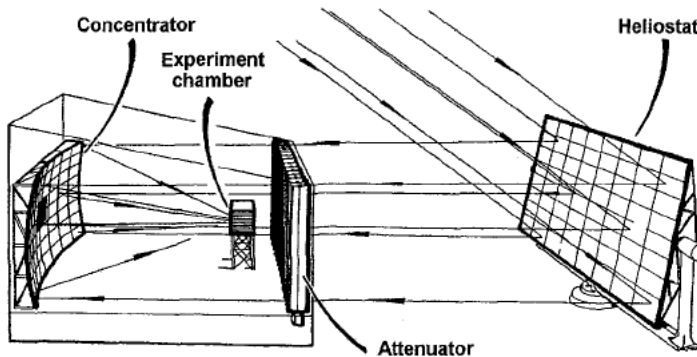


Figure 1 The Odeillo Solar Furnace

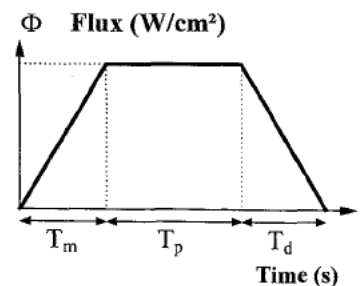


Figure 2 Trapezoidal thermal flux

The position of both subsystems is controlled by a computer which real-time monitors the direct solar illumination ; it allows calibrated heat fluxes to be delivered in a given timing sequence. The maximum flux density obtained in the focal zone was about 550 W/cm², but the use of a second-stage concentrator allowed up to 1200 W/cm² flux on the target. Steel samples were cylinders, 40 mm in diameter and 80 mm in height. One of the plane faces was submitted to the radiant flux, and a water-cooling system, incorporated in the middle of the sample, increased the cooling down speed. Some samples were equipped with intrinsic thermocouples (steel/constantan) set at different depths from the exposed face. A trapezoidal flux shape was used, the raising and falling times being fixed to 0.2 second. Φ represents the flux in W/cm², N the shocks number, T_p the flux plateau duration, T_m the raising time, T_d the falling time, T_r the time between two shocks (see figure 2).

2. A FIRST NUMERICAL SIMULATION

Using a 1-D finite difference scheme (Mur6e), we simulate a thermal shock test on a steel half space, first uncovered and secondly covered by an electrolytic chromium coating. The maximum temperatures on different points in our sample are obtained. During the test, these results are essentially valid along the cylinder axis. This simulation shows us that we must use the second stage concentrator if a high temperature is researched and also if a thermal shock is to be realised. This allows us to avoid too long thermal plateau duration times which may treat the sample.

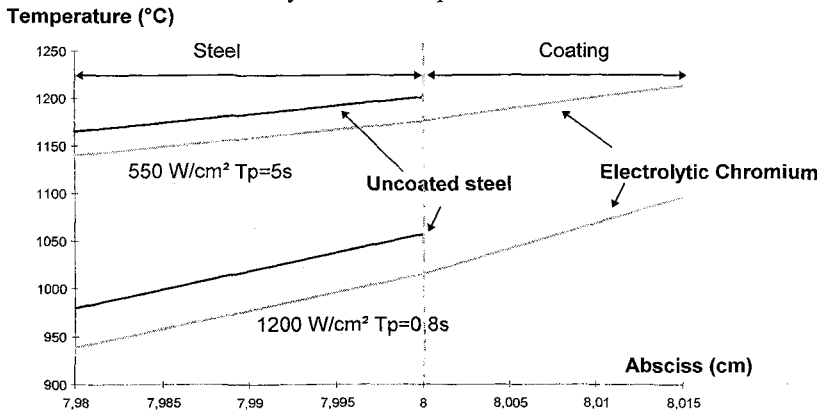


Figure 3 Thermal shock simulation (Mur6e)

3. THERMAL SHOCK ON 35NCDV12 STEEL

A preliminary experimental study was performed on uncoated steel samples. Its first aim was to find the flux level and plateau duration required for generating a thermal affected zone (T.A.Z. : the steel zone in which a phase change occurred by hardening, a martensitic structure is obtained) by applying a single thermal shock. Using the previous numerical simulation results and empirical tests results, the following experimental conditions were chosen and the corresponding T.A.Z. measured.

Table 1 Thermal shocks - Experimental conditions on 35NCDV12 steel

Thermal Flux (W/cm ²)	T _m (s)	T _d (s)	T _p (s)	N	T.A.Z.
1100	0.2	0.2	0.8	1	200μm
1100	0.2	0.2	1.6	1	1.1mm

The temperature field was calculated using either a simplified analytical model, either a preliminary version of 1-D finite difference scheme, either a finite-element thermomechanical code (Abaqus). The measured thermal affected zone depths were also compared to the calculated ones. As it is shown on the following figure, the better correlation between measured and numerical results was obtained when using a temperature dependence of the thermophysical properties : thermal conductivity, specific heat, density. No phase transformation is computed in the code we use.

We choose to compare the area where temperature reaches up to the phase transformation temperature. Obviously this method overestimate the T.A.Z..

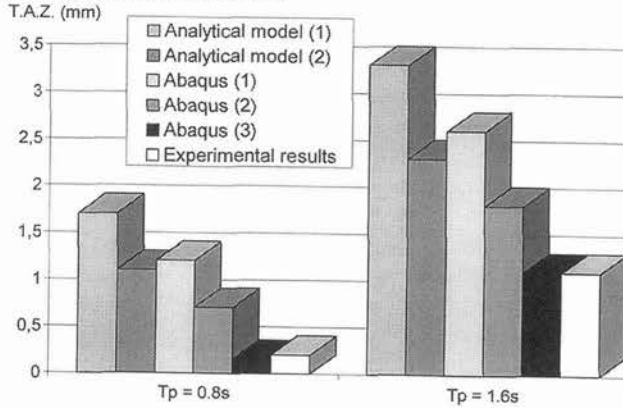


Figure 4 T.A.Z. depths - Comparison experimental results and calculated ones
 (1) constant properties - (2) temperature dependence of the physical properties
 (3) = temperature dependence of the physical properties and absorption on the exposed face fixed to 0.8

4. THERMAL FATIGUE ON AN ELECTROLYTIC CHROMIUM COATING

In a second step the behaviour of electrolytic chromium coatings suffering thermal cycling was investigated. The raising and falling times are still fixed to 0.2 second. The maximum heat flux $\phi=1200\text{W/cm}^2$ is used, and T_r is fixed to 30 second such as the surface temperature reached at each shock would be the same.

In the first hand, using $T_p=0.8\text{s}$ and $N=18$, we observed the various main damage types similar to those observed on the internal surface of gun tubes : chromium recrystallization, some cracking and steel thermal affected zones. Nevertheless no surface cracking network was obtained.

In a second hand such a surface cracking network was obtained using $T_p=0.6\text{s}$ and $N=1000$. Electrolytic chromium deposits [2] elaborated by continuous current (CC) present a columnar growth and a strong $\langle 111 \rangle$ fiber texture that slow sharpen during growth. CC deposits have a microcracks net. After a post-deposition thermal treatment, these cracks are a little enlarged (see figure 5). And after a one thousand thermal shocks cycle the chromium surface presents a second cracking network so that its average size is about $450\ \mu\text{m}$.

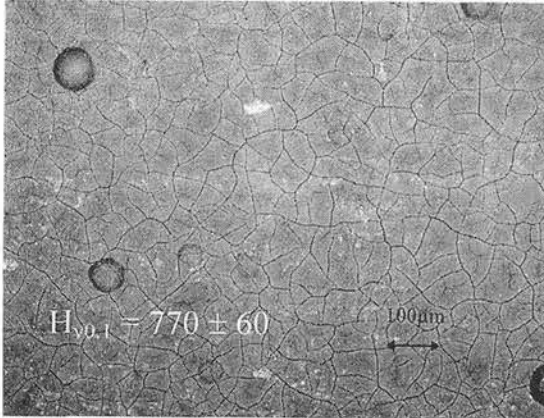


Figure 5 Electrolytic chromium surface after post-coating thermal treatment

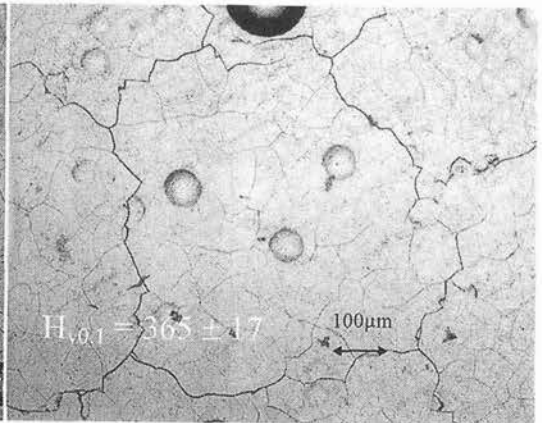


Figure 6 Cracking network after 1000 thermal shocks

5. TEMPERATURE AND STRESS FIELDS IN COVERED AND UNCOVERED SAMPLES SUFFERING A THERMAL SHOCK

Finally the temperature and stress fields are calculated using the finite-element thermomechanical code Abaqus. As we don't know the steel absorption coefficient we chose to simulate a test which has been experimentally carried out on uncovered steel. Thus the following applied conditions are used : $\phi=1100\text{W}/\text{cm}^2$; $T_p=0.8\text{s}$. Mesh tests are carried out such as we reached the limit under which no changes affected the results. Three elements are used in the coating depth and the interface contact was supposed to be perfect. As we say it before, the results are closed to the reality when using a temperature dependence of the thermo-mechanical properties. Therefore we first start calculation tests on uncovered steel using this temperature dependence of the properties (case 2) and only by changing the steel absorption coefficient such as we manage to get the nearer T.A.Z. value really observed in the metallurgical analysis. So the steel absorption is fixed to 0.82 but no temperature dependence has ever been used. In case 1, uncovered steel with constant properties was used. Then we started simulation tests on covered steel by a pure chromium $120\mu\text{m}$ coating. Case 3 used constant properties for both materials. Case 4 used temperature dependence except for chromium Young's modulus and Poisson's ratio. And the last case used a steel temperature dependence and constant electrolytic chromium properties [3,4] as they are currently used. The chromium absorption coefficient [5] was fixed to the constant value 0.86, it is mainly available above 600°C .

For the five cases we use a pure elastic behaviour law. Obviously, the maximum temperatures at the surface and the interface (figure 7) are obtained when the thermal plateau duration is finished, i.e. at $t=1\text{s}$. The temperature difference between the one calculated with constant properties and the one with temperature dependence can reach 100°C . In fact constant properties makes us really overestimate the temperatures reached and therefore also the T.A.Z.. The same T.A.Z. is obtained when using either uncovered or covered steel. It is true either using temperature dependence or not. We only used constant properties for the electrolytic chromium but the results are approximately closed to the pure chromium using temperature dependence.

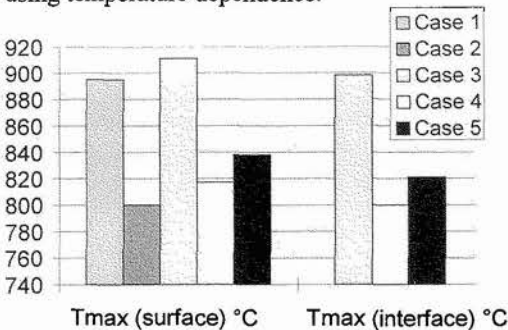


Figure 7 maximum temperatures

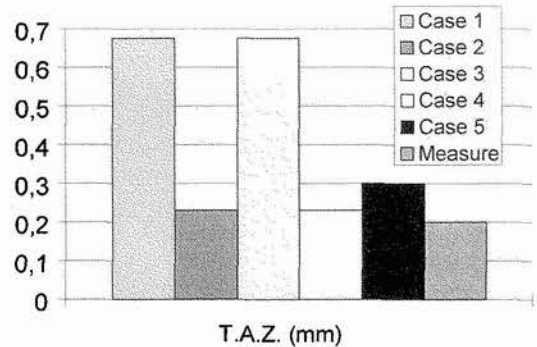


Figure 8 T.A.Z. depths

Figure 9 shows σ_{rr} stresses in uncovered and covered steel samples at the cylinder axis at different depths for each case. When steel is uncovered all stresses are insignificant except σ_{rr} . We find a little shearing for covered steel but the main stress is σ_{rr} . When the sample is suddenly exposed to the heat flux, the centre goes into compression because of its expansion while the remaining material is still cold and unstrained. This is colloquially known as an « upshock » [6]. For uncovered steel with temperature dependence of the properties the surface material gets less into compression than at a larger depth, due to the steel expansion coefficient in temperature. The stresses time evolution in the steel is similar as it is covered or not, either we compare the constant properties using results (figure 9a and 9c) either the temperature dependence using ones (figure 9b and 9d) but they're less compressive when using temperature dependence.

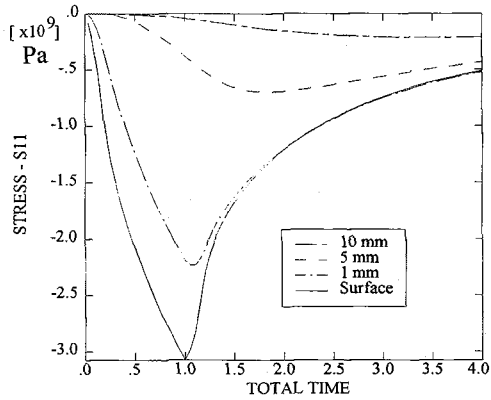


Figure 9a Uncovered steel
Constant thermal and mechanical properties

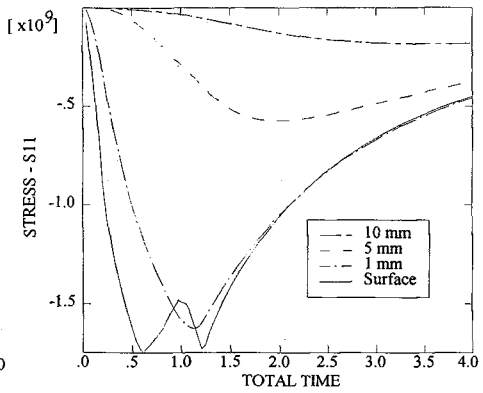


Figure 9b Uncovered steel
Temperature dependence of the thermo-mechanical properties

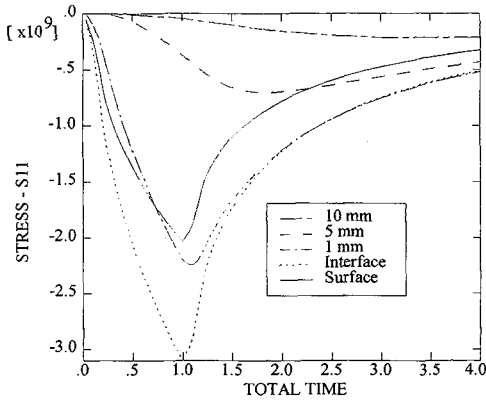


Figure 9c Steel covered by pure chromium
Constant thermal and mechanical properties

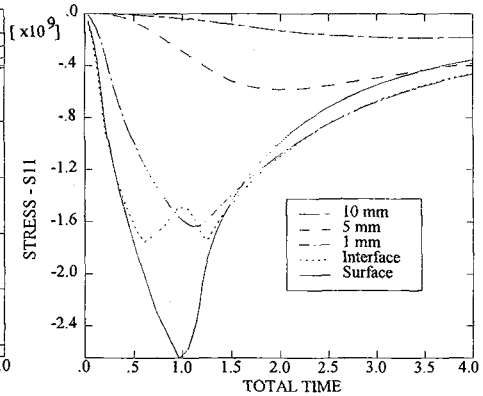


Figure 9d Steel covered by pure chromium
Temperature dependence of the steel thermo-mechanical properties

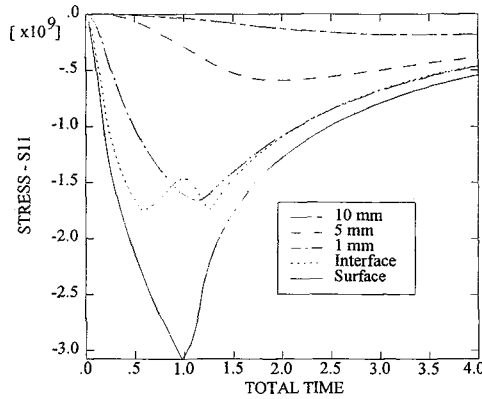


Figure 9e Steel covered by electrolytic chromium
Temperature dependence of the steel thermo-mechanical properties

Figure 9 Stresses in uncovered and covered samples, calculated by a finite element thermo-mechanical code (Abaqus)

Stresses in steel covered by electrolytic chromium don't change but chromium stresses are always more compressive than those in steel.

Plastic zones depths were determined with a Von Mises criterion. They're 30% less important when using temperature dependence.

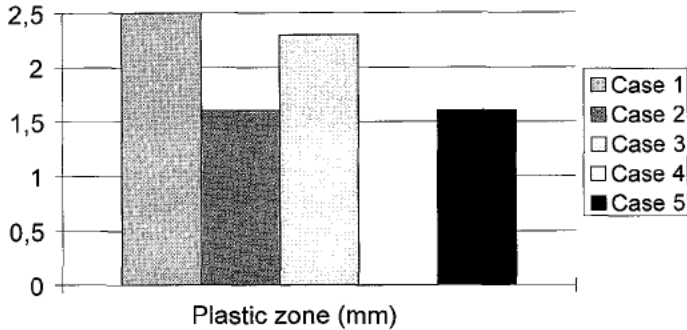


Figure 10 Plastic zones depths calculated with a Von Mises criteria and an elastic behaviour

6. CONCLUSION

This study shows that calculations results are closer to the reality when temperature dependence of the thermo-mechanical properties with steel covered or not by a chromium coating exposed to such thermal shock conditions is used. In particular it induces some variations to the temperatures, the thermal affected zones, the stresses, and the plastic zones. Some material properties in temperature have been measured but all of them aren't known yet. Nevertheless not all of them might be known. Therefore we'll start studying the sensibility of each property so that for instance some of the massif properties could be used instead of the « real ones » without too big calculated values changes. We demonstrated that for such an application, dependence in temperature of much properties must be used.

Acknowledgements

The author are grateful to B. Hosdez (CTA/SMS) for his metallurgical analysis and also to J.M. Sayous (CTA/LOT) for the solar furnace tests.

References

- [1] Suzanne P., J.J. Serra, « Thermal flux measurement methodology and flux sensors calibration at the ETCA solar furnace », Proc. 49th CNATI, Vol.3, pp. 2087-2095 (Perugia I / September 26-30, 1994)
- [2] Cassagne V., « Etude de la croissance de dépôts de chrome électrolytiques - Conséquences sur la structure et l'état mécanique », 1996, Thèse ENSAM
- [3] J.L. Coupeau, P. Sabourin, « Etude du comportement de différents matériaux protecteurs avec le logiciel de simulation de contraintes thermomécaniques à l'intérieur des tubes d'armes », rapport GIAT industries 58547, September 1992
- [4] S. Serror, « Synthèse des connaissances sur l'usure des tubes de canon - Propriétés du chrome électrolytique et mode de dégradation », Rapport ETCA, December 1996
- [5] Incropera F.P., DeWitt D.P., « Fundamentals of Heat and Mass Transfer », Wiley fourth edition, 1996
- [6] R.P. Skelton, « Introduction to thermal shock », High Temperature Technology, Vol 8 No 2 (May 1990), pp 75-88